Comparison of neutral winds and ion drifts Observed at Jang Bogo station, Antarctica

Young-bae Ham(astro422@kopri.re.kr)[1,2], Geonhwa Jee[1,2],
Changsup Lee[1], Hyuck-Jin Kwon[1], Jeong-Han Kim[1], Eunsol Kim[1,5], Nikolay Zabotin[3], Terence Bullett[3], and Qian Wu[4]

[1]Korea Polar Research Institute, Incheon, Korea, [2]University of Science and Technology, Daejeon, Korea,
[3]University of Colorado, Boulder, CO, USA, [4]Naional Center for Atmospheric Research, Boulder, CO, USA, [5]Chungnam National University, Daejeon, Korea

Abstract

A distinct feature of the high latitude ionosphere is the convective motion of plasma which is generally antisunward over the polar cap and sunward in the auroral region. It is well known that this ionospheric plasma convection results in neutral wind patterns that resembles to the plasma convection pattern via ion-neutral collisions. At Jang Bogo station (JBS) which is located mostly within the polar cap, Fabry-Perot Interferometer (FPI) and Vertical Incidence Pulsed Ionospheric Radar (VIPIR) have been simultaneously operated to observe neutral winds and ion drifts, respectively, and the data from these two instruments allow us to directly compare the neutral winds and the ion drifts to investigate their couplings. The results of this comparison show that although there exist similarities in their diurnal variations within the polar cap, the neutral wind vectors follow the ion drift vectors with systematic differences, not only in magnitude but also in the direction. In this study, we present the preliminary results of the simultaneous observations of neutral winds and ion drifts during winter in 2017 at JBS, Antarctica.

High latitude ionospheric and thermospheric dynamics

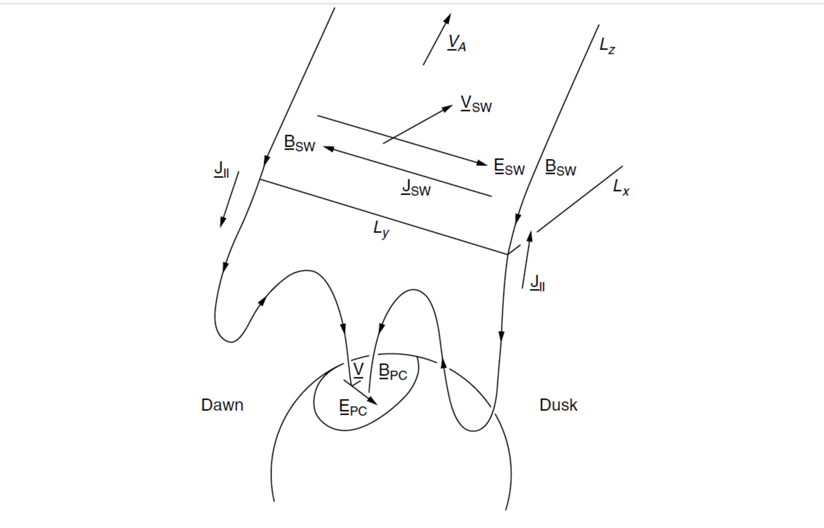

Figure 1. Schematic representation of the magnetic connection between the solar wind dynamo and the ionospheric load.

- Observers in the Earth-fixed coordinates experience an electric field which is given by $\vec{E} = -\vec{V}_{sw} \times \vec{B}$
- This electric field is transmitted to the ionosphere along the highly conducting magnetic field lines.

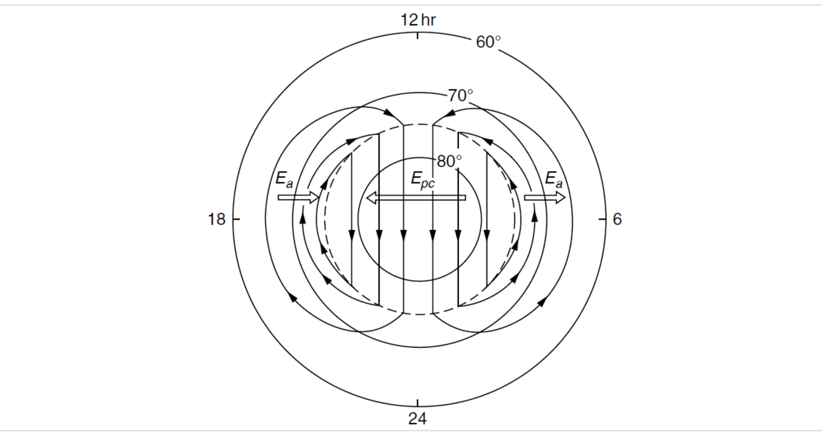

Figure 2. Representation of ionospheric electric fields in the northern hemisphere polar cap and auroral zone, as well as the plasma flow due to those fields.

- This transmitted electric field generates ionospheric convection in the ionospheric heights.
- The motion is antisunward in the polar cap and sunward in the auroral region.
- Via the ion-neutral collision, the plasma motion leads to a acceleration of the neutral atmospheric gases in its direction.
- And this acceleration creates a horizontal wind circulation that corresponds to the ionospheric convection pattern.

$$\rho_n \frac{D\vec{u}}{Dt} = \rho_n \vec{g}^* - \vec{\nabla} p - \rho_n \nu_{in}(\vec{u} - \vec{v}_i) - 2\rho_n \vec{\Omega} \times \vec{u}$$: Momentum equation of neutral gas in the rotating frame

Instruments and data used

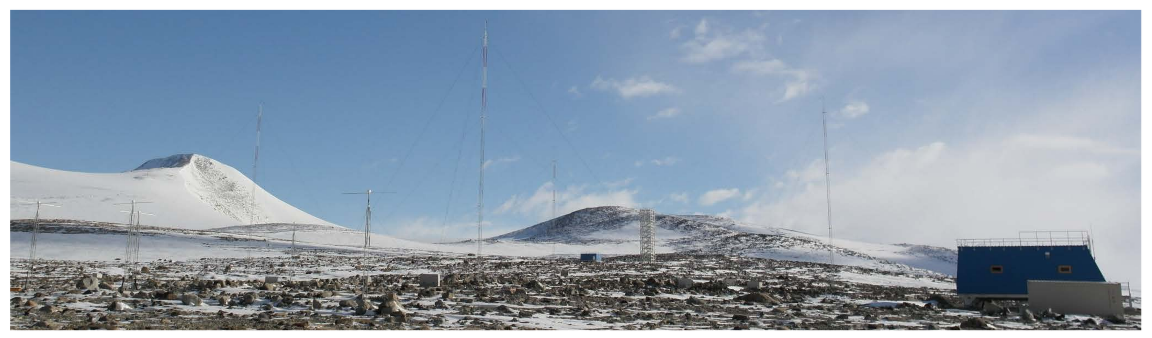

Figure 3. Vertical Incidence Pulsed Ionospheric radar (VIPIR)

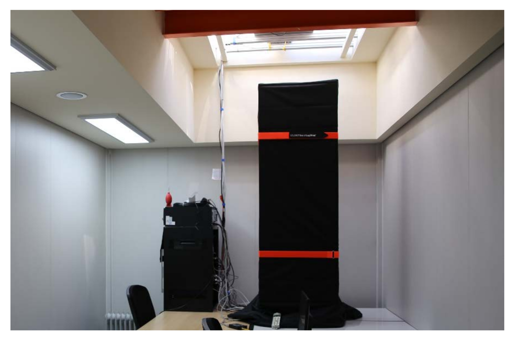

Fig 4. Fabry-Perot Interferometer (FPI)

VIPIR
- Radar instruments that observes the ionosphere by analyzing reflected signals (echoes) from the ionosphere.
- It gives height profiles of the ionosphere by sweeping the transmitting frequency (0.3-26MHz).
- Temporal resolution: ~2 minutes.

FPI
- Optical instruments that observes thermosphere.
- It gives thermospheric winds and temperatures, and these are derived by analyzing measured airglow emissions.
- It targets OH Meinel band (87 km), OI-5577 (97 km), and OI-6300 (250 km) airglows.
- Temporal resolution: ~55 minutes.

- In this study, 250 km ion-drifts (VIPIR) and 250 km neutral winds (FPI) were studied.

Averaged 250 km ion-drifts and neutral winds

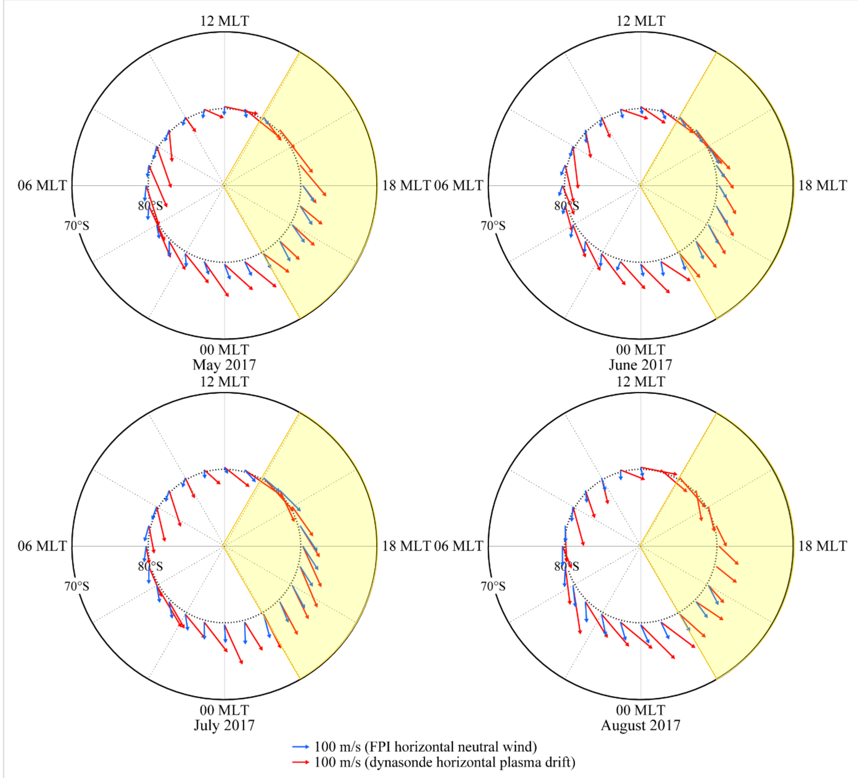

Figure 5. Monthly averaged 250 km ion drifts (red) and 250 km neutral winds (blue).

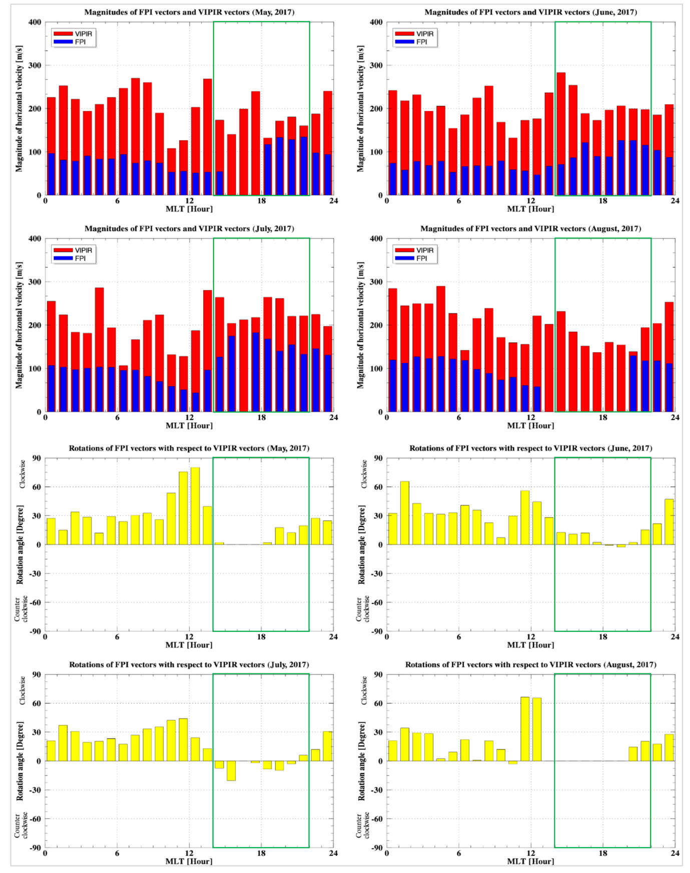

Figure 6. Magnitudes of ion-drift and neutral wind vectors (left), and rotation angles of the neutral wind vectors with respect to ion-drift vectors.

- Magnitudes of neutral wind vectors are smaller than those of ion drift vectors.
- Overall, neutral wind vectors are rotated clockwise with respect to ion drift vectors.
- Directions of neutral wind vectors follow those of ion drifts vectors well during 14~22 MLT.
- Magnitudes of neutral wind vectors show the largest values during this time interval.

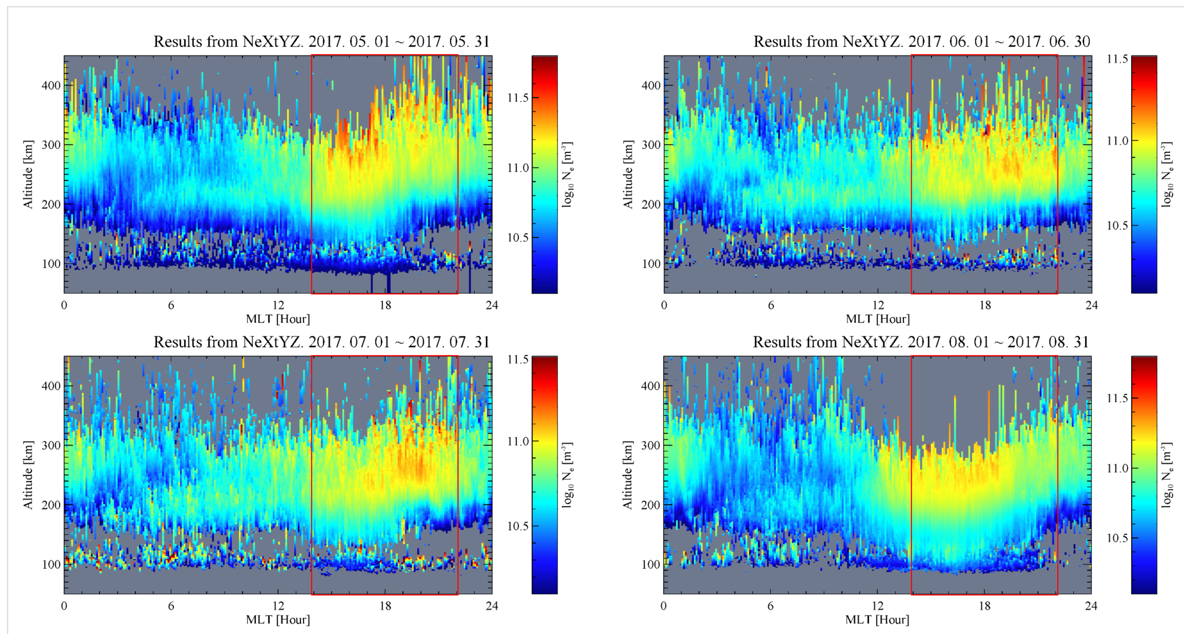

Figure 7. Monthly averaged plasma density profiles.

$\nu_{i,n} \approx 2.6 \times 10^{-9}(n_n + n_i)A^{-1/2}$ (A: The mean neutral molecular mass in atomic mass units)

- ➢ High plasma density during 14~22 MLT results in increase in ion-neutral collision frequency.
- ➢ As a result, neutral gases are easily accelerated in the direction of ion motion during 14~22 MLT.

TIEGCM results

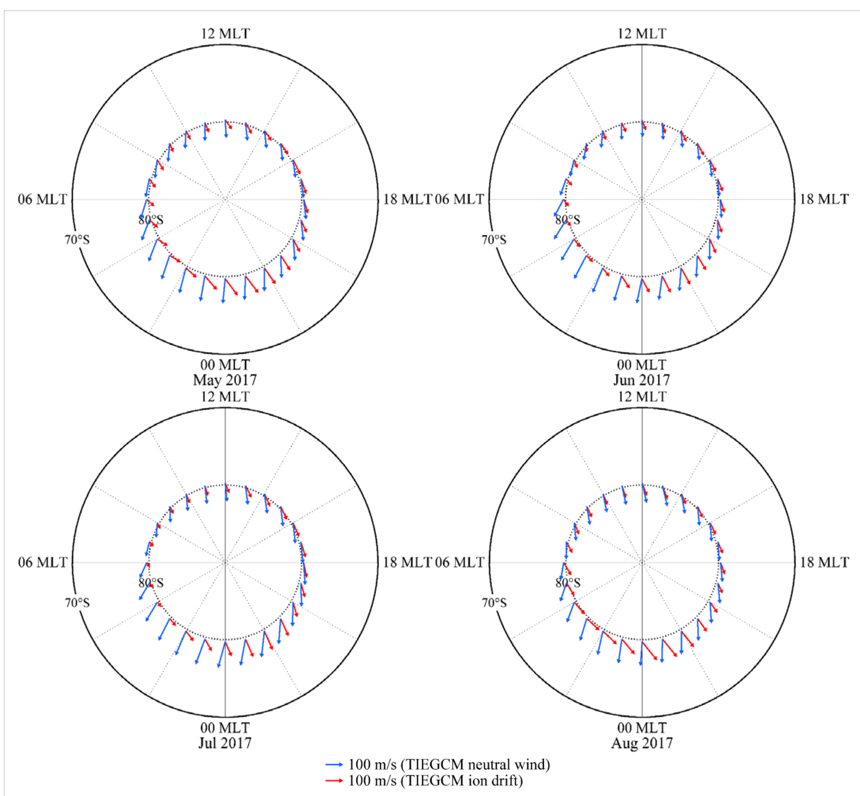

Figure 8. Monthly averaged 250 km TIEGCM ion-drifts and neutral winds.

- Generally, configuration of TIEGCM ion drift and neutral wind vectors looks similar to observations.
- TIEGCM largely underestimates ion drifts.
- TIEGCM slightly overestimates neutral winds.

Response to the IMF variations – Case study

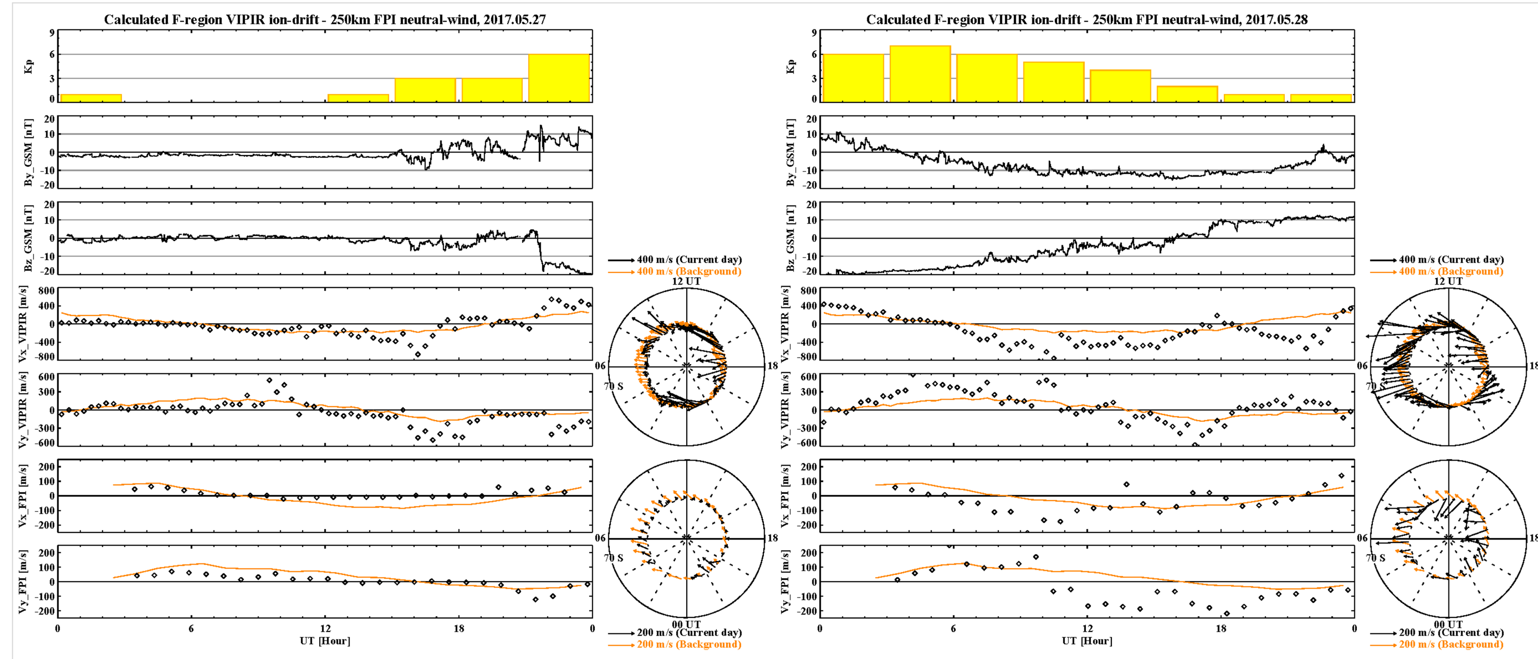

Figure 9. Daily plots of ion drifts and neutral winds data when strong IMF variations appeared. Orange lines indicate 31-day averaged data centered on each day.

- Ion drift measurements showed enhanced convection pattern for the southward IMF turning occurred at about 2230 UT on May 27, and weaken (or reversed) convection pattern for the northward IMF turning occurred at about 1730 UT on May 28.
- It can be explained by the increase of the cross polar cap potential for the increasing southward IMF.
- Neutral wind measurements also showed perturbed signature from the 31-day averaged value for the IMF B_z variations, but it is not easy to interpret intuitively.

▪ **For the IMF B_y variations without significant IMF B_z variations**

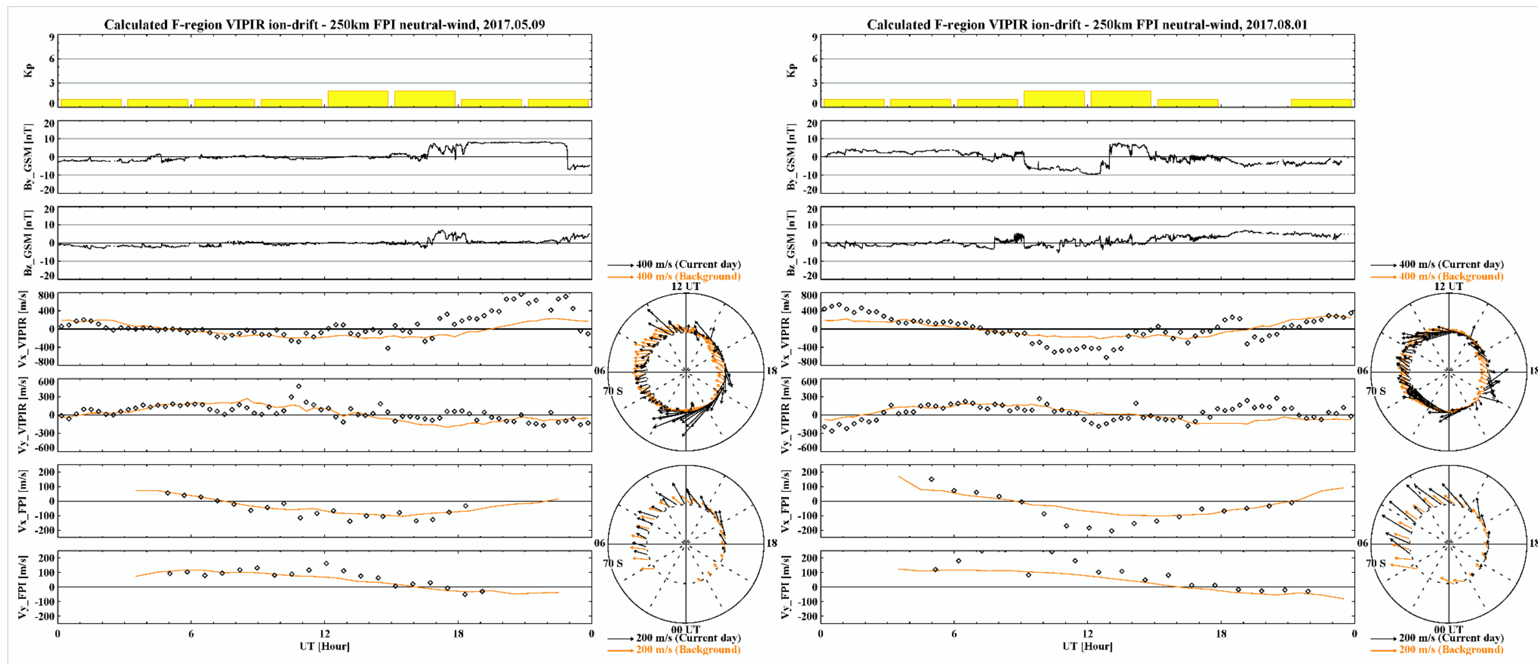

Figure 10. Daily plots of ion drifts and neutral winds data when strong IMF variations appeared. Orange lines indicate 31-day averaged data centered on each day.

- As IMF B_y changed (around 1700 UT on May 09 and 0900 UT on August 01), ion drift measurements showed clear changes.
- On August 01, changes in neutral wind measurements were also identified. But the meridional component changes occurred prior to the IMF B_y variations, thus in this case, it's not clear whether the variations in the meridional component are directly related to the IMF B_y variations.

Summary and conclusion

- There exist systematic differences between the direction of neutral winds and ion drifts.
- The neutral winds are determined by the ion drag force as well as other forces (e.g., pressure gradient force).
- During 14 ~ 22 MLT sector, the differences between the neutral wind vectors and ion drift vectors are minimized not only in the direction but also in the magnitudes.
- During this magnetic local time sector, the large plasma density enhances the ion-neutral collision frequency and thereby increases the ion drag force.
- NCAR TIEGCM model results showed similar ion drift and neutral wind patterns to the observations, but there is a significant underestimation of ion drifts, which is even smaller than neutral winds.
- When the IMF conditions varied the measurements of ion drift also showed the corresponding changes, but it was difficult to see such changes in the neutral wind measurements.

Future work

- Temporal resolution of FPI wind measurements will be improved from 55 min. to 15 min.
- FPI and VIPIR observations are continuously performed for a long-term observation to further investigate the ion-neutral interactions.